

Dalton Transactions

An international journal of inorganic chemistry

Accepted Manuscript

This article can be cited before page numbers have been issued, to do this please use: J. Ahmad, A. P. Atencio, J. S. Ward, M. Engeser, K. Rissanen, I. Angurell and L. Rodriguez, *Dalton Trans.*, 2026, DOI: 10.1039/D6DT00964F.



This is an Accepted Manuscript, which has been through the Royal Society of Chemistry peer review process and has been accepted for publication.

Accepted Manuscripts are published online shortly after acceptance, before technical editing, formatting and proof reading. Using this free service, authors can make their results available to the community, in citable form, before we publish the edited article. We will replace this Accepted Manuscript with the edited and formatted Advance Article as soon as it is available.

You can find more information about Accepted Manuscripts in the [Information for Authors](#).

Please note that technical editing may introduce minor changes to the text and/or graphics, which may alter content. The journal's standard [Terms & Conditions](#) and the [Ethical guidelines](#) still apply. In no event shall the Royal Society of Chemistry be held responsible for any errors or omissions in this Accepted Manuscript or any consequences arising from the use of any information it contains.

Triphenylene Chromophore Enhances Emission in Au/Cu Heterometallic Complexes

Jalal Ahmad^a, Anyie P. Atencio^a, Jas S. Ward,^b Marianne Engeser,^c Kari Rissanen,^b
Inmaculada Angurell^a and Laura Rodríguez^{a,*}

^a *Departament de Química Inorgànica i Orgànica, Secció de Química Inorgànica, Universitat de Barcelona and Institut de Nanociència i Nanotecnologia (IN2UB). Martí i Franquès 1-11, E-08028 Barcelona, Spain. e-mail: laurarodriguezr@ub.edu*

^b *University of Jyväskylä, Department of Chemistry, 40014 Jyväskylä, Finland.*

^c *Kekulé-Institut für Organische Chemie und Biochemie der Universität, Gerhard-Domagk-Strasse 1, D-53121 Bonn, Germany.*

Abstract

Heterometallic Au(I)–Cu(I) assemblies are attractive luminescent platforms due to synergistic metallophilic interactions and enhanced spin–orbit coupling. We report a new family of Au(I)–Cu(I) complexes incorporating a rigid 2-ethynyltriphenylene chromophore and a pyridyldiphenylphosphine auxiliary ligand. Stoichiometric reactions between a mononuclear alkynyl gold(I) precursor and Cu(I) salts bearing different counterions (PF₆[−], OTf[−], BF₄[−]) afford Au₂Cu₂ assemblies whose structures and packing are strongly counterion-dependent. Single-crystal X-ray diffraction reveals Au–Cu interactions supported by Cu–N(pyridyl) and Cu···π(alkynyl) contacts. The photophysical studies show counterion-modulated dual fluorescence/phosphorescence emission in solution, with phosphorescence enhanced under inert conditions. Upon immobilization in polymer matrices, all heterometallic complexes display efficient room-temperature phosphorescence with quantum yields up to 40% and millisecond lifetimes. These results highlight the role of counterions and matrix rigidification in controlling excited-state deactivation in heterometallic coinage-metal systems.

Keywords: heterometallic systems; luminescence; clusters; X-ray crystallography; supramolecular assemblies



Introduction

Heterometallic coinage-metal clusters, particularly those combining gold(I) and copper(I), continue to attract considerable attention due to their intriguing photophysical properties arising from metallophilic interactions and ligand–metal cooperativity. The d^{10} – d^{10} contacts between Au(I) and Cu(I) centres not only stabilize unusual architectures but also modify significantly their photophysical properties promoting efficient spin-orbit coupling (SOC), enabling room-temperature phosphorescence (RTP) and thermally activated delayed fluorescence (TADF).¹⁻¹³ The development of new materials containing both metallophilic interactions and specific chromophores allow the fine tuning of the resulting luminescent properties. Hence, Au–Cu systems appear as promising candidates for light-emitting devices, sensors, and photocatalytic singlet oxygen generation.^{1,14-17}

Recent studies have demonstrated the potential of chiral and polynuclear Au–Cu(I) assemblies stabilized by phosphine or N-heterocyclic carbene ligands to deliver intense and tunable emissions. For example, chiral NHC-stabilized Au(I)–Cu(I) clusters have achieved exceptional circularly polarized luminescence and EQE values up to 20.8% in CP-OLEDs,¹⁵ while other Au_2Cu_2 and Au/M heterometallic systems display near-unity photoluminescence quantum yields and microsecond-scale phosphorescence lifetimes, evidencing the strong influence of metal–metal coupling on excited-state dynamics.^{16,18-20} Moreover, the photophysical response has been shown to depend critically on counterions and crystal packing, which modulate intermolecular π – π interactions and metallophilic contacts.^{2-4,17-19}

The incorporation of extended aromatic chromophores, such as polycyclic acenes or triphenylene derivatives, provides an effective strategy to enhance the intraligand (IL) absorption and emission characteristics while promoting π -stacking in the solid state.²¹ Triphenylene, with its rigid planar structure and high photostability, can act as both a light-harvesting antenna and a scaffold for supramolecular organization, favouring aggregation-induced emission (AIE) and energy migration phenomena.^{22,23} Despite these advantages, Au–Cu clusters supported by triphenylene-based alkynyl ligands remain unexplored, particularly regarding the interplay between ligand rigidity, counterion identity, and luminescent behaviour.



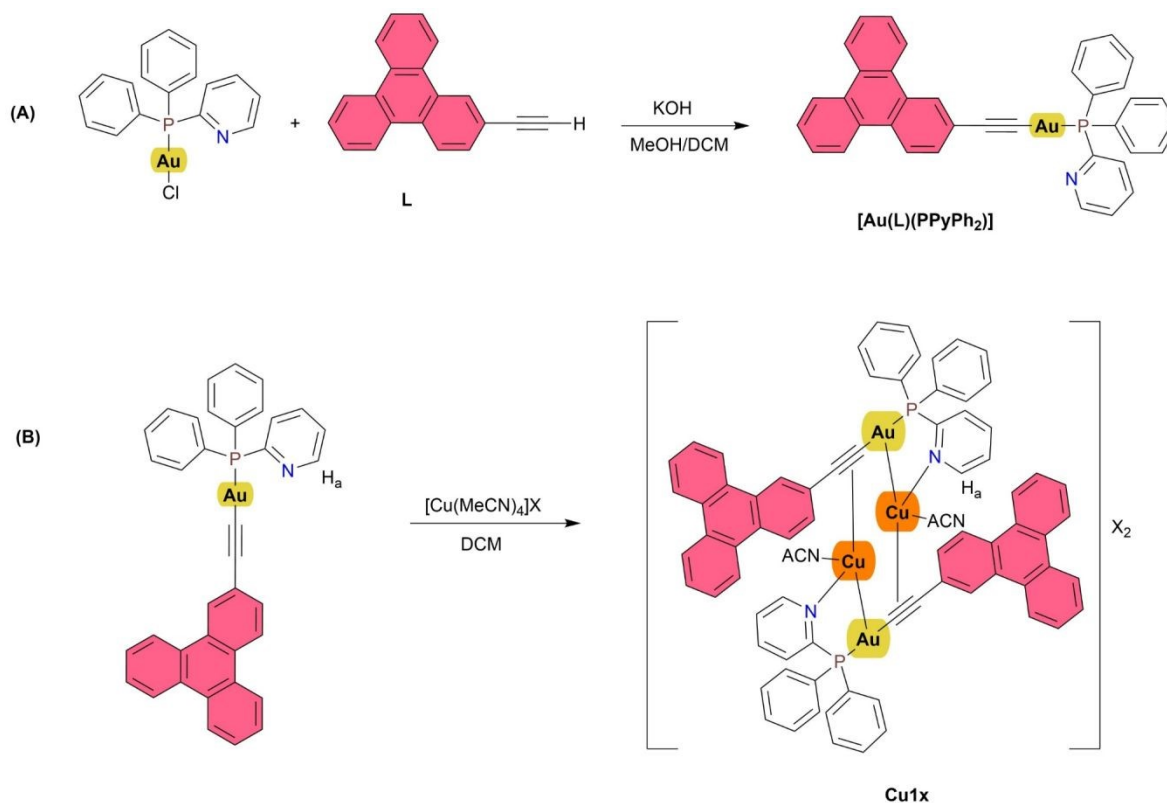
In this work, we report the synthesis, structural characterization, and photophysical properties of a new family of Au(I)–Cu(I) heterometallic complexes incorporating a 2-ethynyltriphenylene chromophore and the pyridyldiphenylphosphine (PPh₂Py) auxiliary ligand. These systems form Au₂Cu₂ cores linked through Cu–N(pyridyl) and Cu··· π (C \equiv C) interactions, with the overall structure and packing modulated by the counterion (PF₆[−], OTf[−], or BF₄[−]). The different size and shape of these counterions have been previously observed to affect the resulting structure and luminescent properties¹⁶; therefore, further investigation in this field is warranted. The combination of a rigid π -conjugated chromophore and metallophilic Au–Cu contacts provide a versatile platform to probe structure–property relationships in luminescent heterometallic clusters. Comprehensive photophysical studies, both in solution and in polymer matrices, reveal counterion-dependent dual emission and efficient phosphorescence under deoxygenated conditions, contributing to the understanding of excited-state dynamics in coinage-metal assemblies.

Results and Discussion

Synthesis and characterization

Three different Au(I)–Cu(I) heterometallic structures were synthesized by the reaction of the previously synthesized [Au(L)(PPyPh₂)] gold(I) complex and different Cu(I)X salts (X = PF₆[−] (a), OTf[−] (b) and BF₄[−] (c) (Scheme 1). The gold complex contains the 2-ethynyltriphenylene as chromophore (L) and the pyridyldiphenylphosphane as ancillary ligand, having the pyridyl unit to coordinate to the second metal center (Schemes S1 and S2). The formation of the gold(I) complex was evidenced by the disappearance of the terminal alkynyl proton in the corresponding ¹H NMR spectrum and a 10 ppm downfield shift in the ³¹P{¹H} NMR spectra (see SI). The synthesis of the final Au(I)/Cu(I) heterometallic structures was carried out by the stoichiometric reaction of [Au(L)(PPyPh₂)] with the corresponding [Cu(MeCN)₄]X salt in dichloromethane overnight at room temperature (Scheme 1B) obtaining orange-red solids with moderate yields. ¹H, ¹⁹F, and ³¹P{¹H} NMR and IR spectroscopies together with electrospray ionization mass spectrometry (ESI-MS) in positive and negative mode demonstrate in all cases the formation of the compounds depicted in Scheme 1 (Fig. S1-S29).





Scheme 1. Synthesis of the gold(I) precursors (A) and their Cu(I)/Au(I) derivatives (B). X= PF_6^- (a), OTf^- (b), BF_4^- (c). ACN: acetonitrile molecules.

The ^1H NMR spectra show that the protons in the *ortho* position (H_a) to the nitrogen atom in the pyridyl ring of the phosphine are affected by the coordination of the Cu(I) center in all the cases with a 0.5-0.9 ppm downfield shift with respect to $[\text{Au}(\text{L})(\text{PPyPh}_2)]$ (see SI). The broadening and downfield shift observed for the heterometallic systems is attributed to the repolarization of the heterometallic product of SOC influenced, as previously observed in other systems previously studied in the research group.¹⁶ A solvent molecule (acetonitrile) is occupying the fourth coordination position of the pseudo-tetrahedral Cu(I) center (see Fig. S7), due to the weak coordination ability of counteranions. This solvent molecule can be replaced by water or PF_2O_2^- formed by partial hydrolyzation of PF_6^- during the crystallization process (see below X-ray crystal structure of **Cu1a** and **Cu1b**). The $^{31}\text{P}\{^1\text{H}\}$ NMR spectrum exhibits a downfield shift of approximately 0.3 ppm in **Cu1b**, and 7 ppm in **Cu1a** and **Cu1c**, with respect to the gold(I) precursor due to the proximity of the phosphorous atom to the Cu(I) coordination site (Fig. S14, S16). The presence of the PF_6^- counterion in **Cu1a** is



evidenced by the septuplet at -144.3 ppm ($^1J_{\text{PF}} = 707$ Hz). The IR spectra of the heterometallic systems display very weak and broad $\nu(\text{C}\equiv\text{C})$ vibrations, a sign of $\text{Cu}\cdots\pi(\text{C}\equiv\text{C})$ coordination being present.

High resolution mass spectra show evidence for the formation of the tetranuclear compounds ($\text{Au}_2\text{Cu}_2\text{L}_2$) in all cases with a signal for a cation $[\text{M}-\text{anion}]^+$ and a series of fragments thereof. ESI spectra recorded under soft conditions additionally show some unspecific aggregation to polynuclear gold complexes, and the spectra are dominated by a strong signal for the cationic diphosphane complex $\text{Au}(\text{PPyPh}_2)_2^+$, both observations are very typical for ESI mass spectra of solutions containing gold(I) and phosphanes (Fig. 1 and S25-S29).

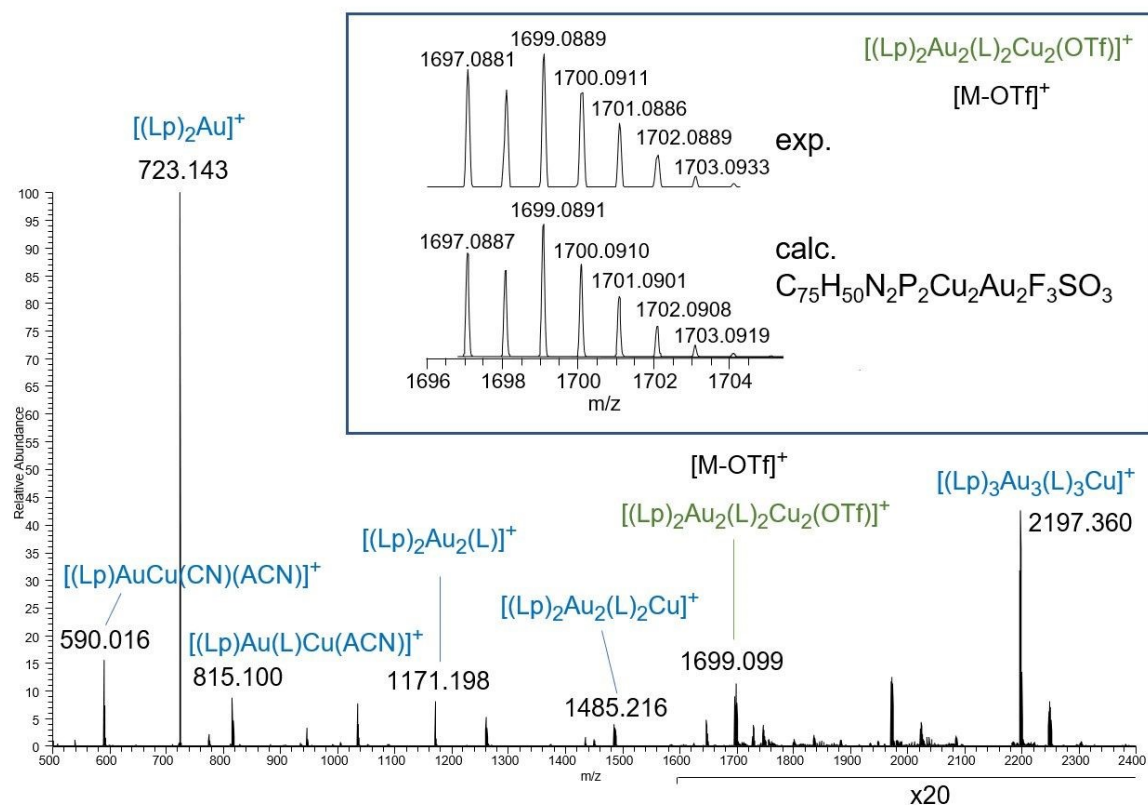


Fig. 1 HR-ESI(+) mass spectra of **Cu1b**, Lp = PPyPh₂.

Single-crystal X-ray diffraction provided the final and unambiguous structural information for $[\text{Au}(\text{L})(\text{PPyPh}_2)]$ and the heterometallic systems **Cu1a** and **Cu1b**. The corresponding structures are presented in Fig. 2, 3 and S30-S33 and the selected bond lengths and angles are summarized in Table S1. The packing of the $[\text{Au}(\text{L})(\text{PPyPh}_2)]$ complex is governed by



C–H $\cdots\pi$ interactions between the triphenylene aromatic unit and a phenyl ring of a neighboring molecule. No aurophilic interactions are observed (minimum Au \cdots Au distances of 5.21 Å, Table S1). The structure of **Cu1a** and **Cu1b** shows a heterometallic Au/Cu core where two Au–Cu direct metallophilic interactions (with Au \cdots Cu distances in the range of 2.77–2.89 Å, Table S1) are interconnected through a PF₂O₂[−] molecule in **Cu1a** and a H₂O molecule in **Cu1b**, incorporated during the crystallization process by displacement of the position occupied by acetonitrile (see above, NMR). Hydrolyzation of PF₆[−] ion is a common feature in coordination chemistry and is very difficult to avoid even working under rigorous inert atmosphere conditions. Certain metal salts, including Cu(I), are capable of catalyzing this hydrolysis in the presence of traces of water.^{24,25} The copper atoms are coordinated simultaneously to the Au(I) center and nitrogen atom of the pyridyl unit of one molecule and an acetylide (Cu $\cdots\pi$ (C \equiv C) interactions) of a neighboring gold(I) unit (Fig. 2). The bond distances between Cu and the centroid of the triply bonded carbon atoms (Cu–C \equiv C_{centroid}) were 1.906/1.917/1.918/1.931 Å (**Cu1a**) and 1.943/1.947 Å (**Cu1b**). The difference on the bridging ligand (OH₂ in **Cu1a** vs PF₂O₂[−] in **Cu1b**) does not affect the presence of metal \cdots metal contacts, that is the main point on the resulting luminescence but provokes slight differences in the general packing.

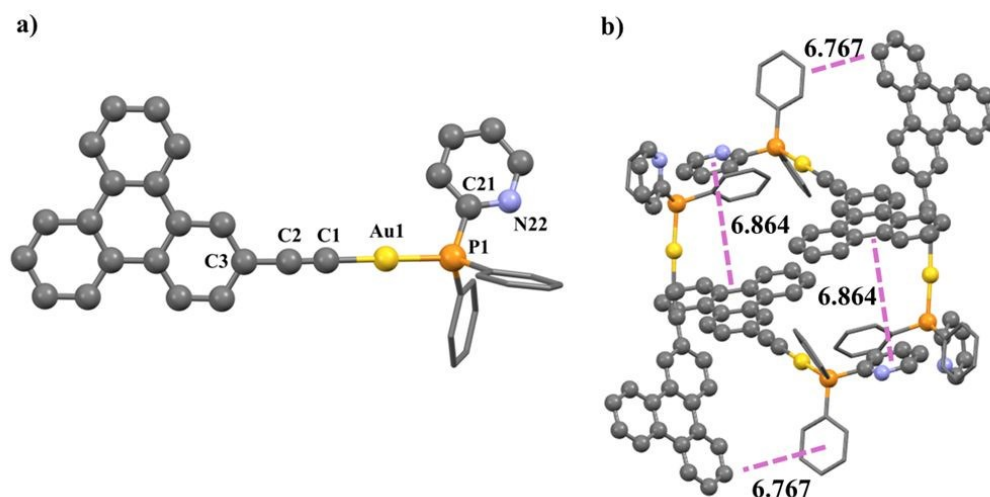


Fig. 2 a) X-ray crystal structures of [Au(L)(PPyPh₂)]; b) Unit cell of the complex. Yellow: gold; orange: phosphorus; blue: nitrogen. Hydrogen atoms have been omitted for clarity. Purple dashed lines indicate π – π interactions. Distances are indicated in Å and have been calculated between ring centroids.



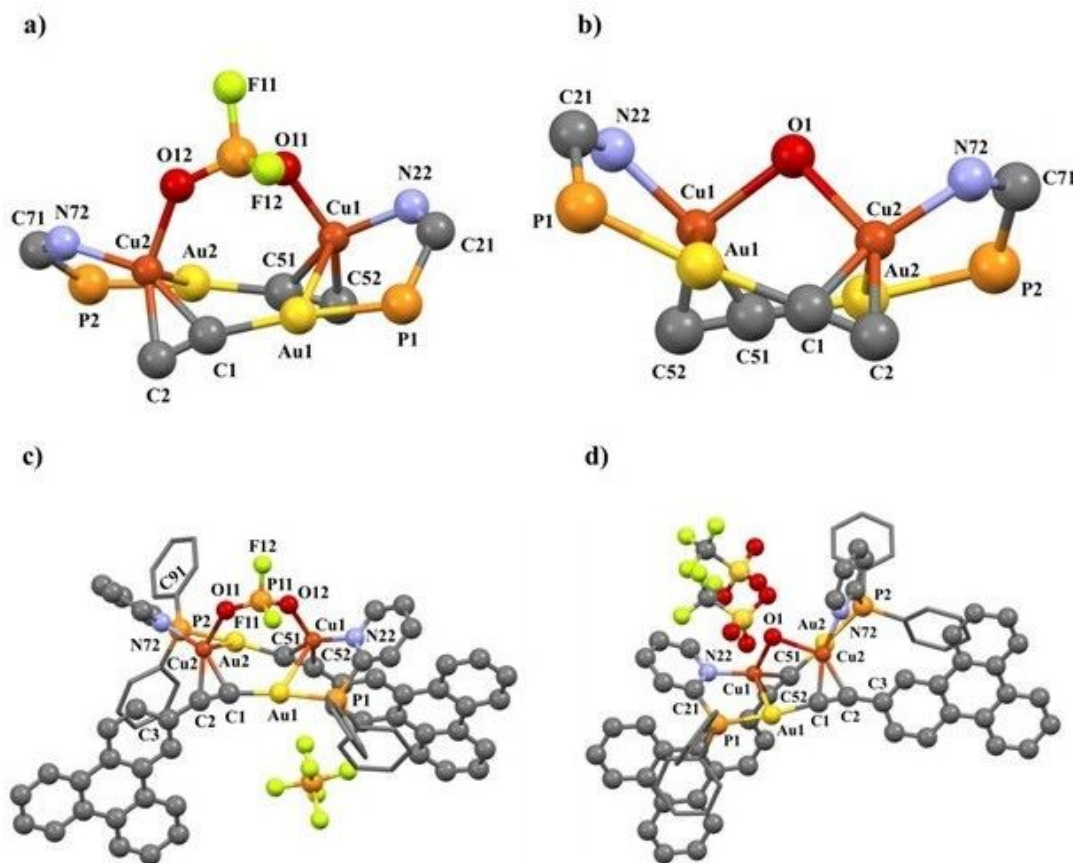


Fig. 3 Heterometallic core of **Cu1a** (a) and **Cu1b** (b). Structure of **Cu1a** (c) and **Cu1b** (d). Yellow: gold; bronze: copper; orange: phosphorus; blue: nitrogen; light green: fluorine. Hydrogen atoms have been omitted for clarity.

Linear coordination of the ligands at the Au(I) centers is preserved, with P–Au–C angles of 170.08(13)/173.43(13)/173.92(15)/174.83(16)° and 174.89(12)/175.23(11)° for **Cu1a** and **Cu1b**, respectively. The angles of the C–Au–Cu bridge of 103.85(16)/106.39(15)/108.32(13)/108.72(13)° in **Cu1a** are noticeably wider than those of 92.42(11)/92.76(11)° in **Cu1b**. These angles differences are responsible for the differences observed in the packing with a less constrained structure in the case of **Cu1b**, while $\pi \cdots \pi$ stacking between the triphenylene groups together with and C–H $\cdots\pi$ interactions between a π ring of the chromophore and the phosphine moieties is observed for **Cu1a**, giving rise to a closer packing arrangement (Fig. 3 and S31–S32). The observed packing arrangement is analogous to the previously obtained with the similar compounds containing phenanthrene



instead of triphenylene, compatible with the presence of a large chromophore that prevents a larger number of metallophilic contacts and the formation of a larger cluster structure.¹⁶

In the **Cu1a** structure, two of the four crystallographically independent triphenylene chromophore units exhibit intermolecular π - π interactions with distances of 3.34 and 3.39 Å between the calculated planes of the triphenylene substituents, and centroid-to-centroid distances of 4.84 and 5.31 Å, respectively. In the case of **Cu1b**, the same intermolecular π - π interaction was present for both of the crystallographically independent triphenylene chromophore units with a centroid-to-centroid distance of 3.74 Å (Fig. S33).

Unfortunately, we could not grow single crystals suitable for X-ray diffraction for **Cu1c** but HR-MS spectrum (Fig. S28 and S29) displays the same pattern than for the other two complexes, supporting the formation of an analogous heterometallic complex with the counterion BF_4^- . Therefore, this does not necessarily constitute a limitation for conducting the corresponding luminescence studies in all cases.

Photophysical Properties

The absorption spectra of the $[\text{Au}(\text{L})(\text{PPyPh}_2)]$ and the corresponding Au(I)-Cu(I) heterometallic systems were recorded in 1×10^{-5} M CH_2Cl_2 solutions at room temperature, as shown in Table 1 and Fig. S34.

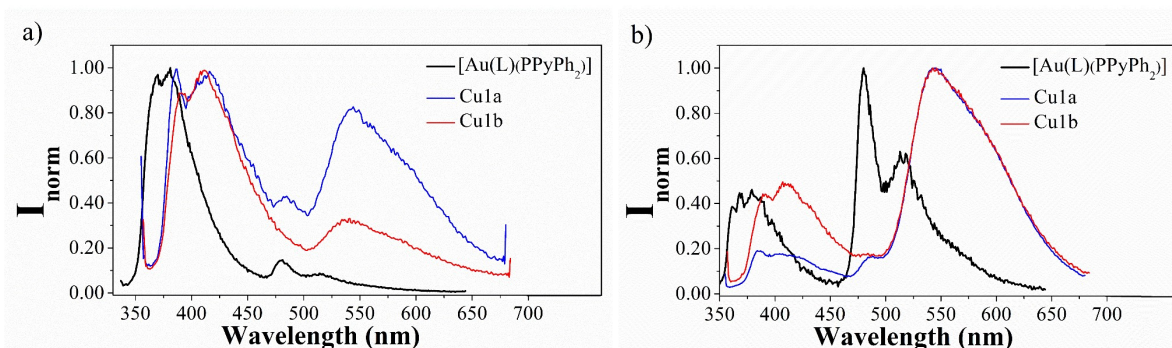
The absorption of $[\text{Au}(\text{L})(\text{PPyPh}_2)]$ exhibits vibronically structured bands corresponding to the alkynyltriphenylene chromophore^{20,26} with peaks at around 268 nm and 318 nm attributed to π - π^* intraligand transitions. The vibronic resolution is lost in the Au(I)-Cu(I) heterometallic structures due to the coordination of the second metal center (Cu(I)) to the alkynyl moiety. The observed broadening can be attributed to the existence of metallophilic contacts and the consequent cluster-centred (^3CC) transitions or ligand-to-metal charge transfer (LMCT) contributions.^{16,27} This band is significantly less intense for **Cu1c**, likely due to its lower solubility in this solvent, which led us to investigate its photophysical properties only in the solid state.



Table 1 Absorption and emission data of the complexes in dichloromethane at 1×10^{-5} M in air-equilibrated conditions and N_2 -saturated conditions

Complex	Absorption λ_{max} , nm ($\epsilon \times 10^4$ M $^{-1}$ cm $^{-1}$)	Fluorescence emission λ_{max} (nm)	Phosphorescence emission λ_{max} (nm)	I_{Phos}/I_{Fl} (air)	I_{Phos}/I_{Fl} Sat- N_2
[Au(L)(PPyPh ₂)]	257 (6.83), 268 (0.78), 277 (7.83), 310 (3.96), 327 (5.19)	379	481	0.1	2.2
Cu1a	259 (6.00), 268 (5.99), 326 (2.39), 346 (2.44)	416	545	0.8	5.7
Cu1b	258 (8.15), 268 (8.09), 327 (2.97), 347 (3.01)	411	537	0.3	2.0

Emission spectra were recorded for all the complexes in solution at room temperature and they display dual emission (Fig. 4). Fluorescence emission at *ca.* 380 nm is recorded for [Au(L)(PPyPh₂)] and is *ca.* 30 nm red-shifted for the heterometallic complexes. A second emission at longer wavelengths is recorded in all cases, with higher intensity for the heterometallic compounds that, as expected, becomes more important upon deoxygenation of the solutions (Fig. 4b). These bands are assigned to metal-perturbed IL emissions for [Au(L)(PPyPh₂)] (¹IL and ³IL respectively) located at the ethynyltriphenylene unit, in agreement with the recorded Stokes' shift and emission lifetimes in the order of a few ns (fluorescence band) and microseconds (phosphorescence band), Table S4.^{20,28-30}

**Fig. 4** Normalized emission spectra of the complexes in a) air-equilibrated conditions; b) N_2 -saturated conditions at 1×10^{-5} M dichloromethane solutions, $\lambda_{exc} = 345$ nm.

The broadening of the lower energy emission band in the heterometallic complexes together with the recorded red-shift with respect to the Au(I) precursor, let us expect a different origin, as previously observed with other Au/Cu heterometallic structures containing the same PPyPh₂ phosphane. These transitions have been attributed to a combination of IL/LL'/LAuMCT excited states origin.¹⁷ In particular, the ligand-to-metal charge-transfer nature of these transitions has previously been assigned on the basis of time-dependent density functional theory (TDDFT) calculations. Moreover, this charge-transfer contribution was found to be enhanced in the heterometallic compounds compared to the homometallic analogues, highlighting the key role of the copper centre, being in agreement with the recorded red-shift.^{17,31,32}

The major contribution of phosphorescence recorded for **Cu1a** with respect to **Cu1b** may be ascribed to the more compact packing (according to X-Ray crystal data) and the slightly shorter distance between the Cu and the alkynyl moiety of the chromophore, favoring the heavy atom effect and intersystem crossing.

The compounds are weakly emissive in the solid state with a main contribution of fluorescence for [Au(L)(PPyPh₂)] and almost pure room temperature phosphorescence for the three Au/Cu complexes with broad shape due to the formation of aggregates (Fig. S35 and Table S6).

The emission properties of the compounds were improved when they are immobilized in organic matrixes, due to the restriction of the non-radiative deactivation pathways.³³⁻³⁶ Additionally, this method allows the samples to be more dispersed, preventing the strong aggregation observed in the solid state and leading to better-resolved spectra with enhanced emission efficiency. Polystyrene, PS, and poly(methyl methacrylate), PMMA were then doped with 1% of the compounds. It was observed in all cases either pure room temperature phosphorescence, that is the emission band at longer wavelengths, *ca.* 550 nm (in PMMA) or major component of this emission (PS) being fluorescence almost negligible in all cases upon deoxygenation of the samples, due to the phosphorescence enhancement (Fig. 5 and Table S7). The emission efficiency has been clearly improved upon to 30-40% in PMMA (Table S8), which is larger than others previously investigated in our group for gold(I) and Au-Cu structures.¹⁷ Very long emission lifetimes have been recorded of hundreds of μ s (Table



S9), which are longer in the order of previously reported heterometallic Au/M (M = Cu, Ag) clusters.^{17,37-42}

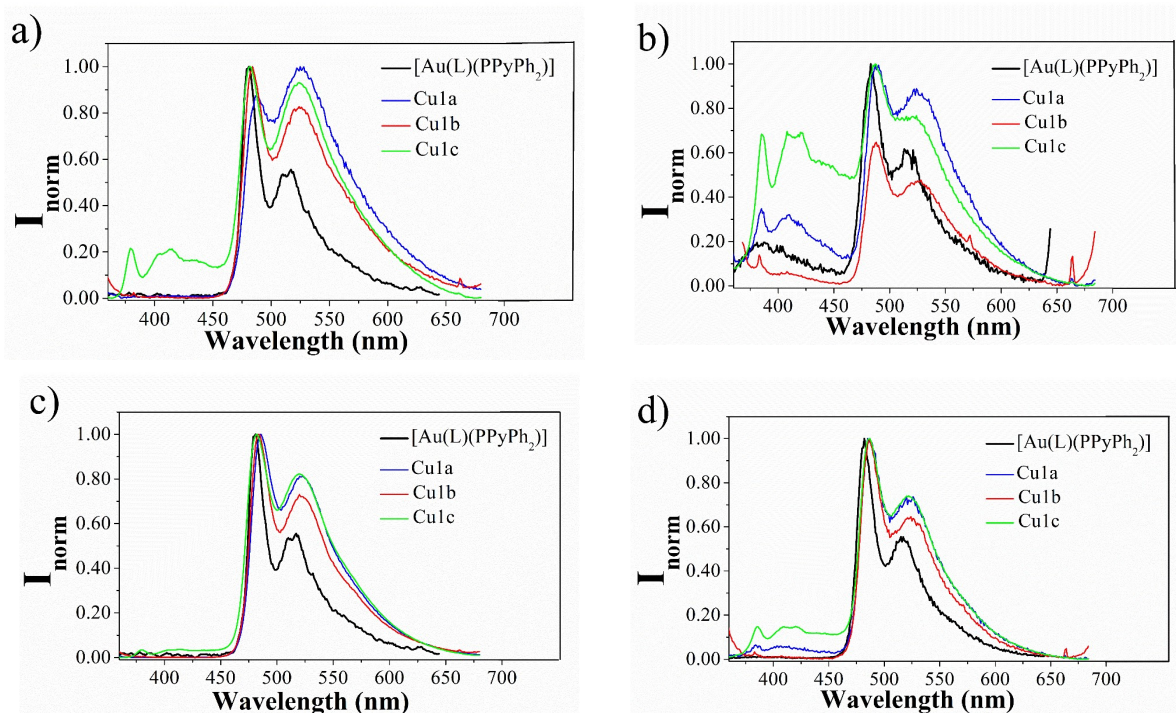


Fig. 5 Normalized emission spectra of complexes in air-equilibrated conditions in a) PMMA matrix; b) PS matrix; and under N₂-saturated conditions in: c) PMMA matrix; d) PS matrix.

Conclusions

The formation of discrete Au₂Cu₂ assemblies is promoted by the cooperative coordination of the pyridyl and alkynyl fragments to Cu(I), together with Au–Cu metallophilic interactions. The resulting stoichiometry of the complexes are induced by the large size of the ethynyltriphenylene chromophore. Single-crystal X-ray diffraction reveals that the counterion plays a decisive role in determining the overall molecular arrangement and intermolecular packing, modulating π – π interactions between triphenylene units and the accessibility of the metallic core.

Photophysical investigations highlight the impact of heterometallic coupling on the excited-state behavior. While weak emission is recorded in dichloromethane solution, this property is clearly enhanced by restriction of non-radiative deactivation channels upon immobilization



of the samples in PMMA and PS matrixes. This immobilization allows an enhancement of the phosphorescence emission quantum yield in a factor of 10x (from 4 to 40%) and very long emission decaytimes up to hundreds of μs .

Interestingly, the use of triphenylene chromophore has induced a clear advantage on the development of efficient room temperature phosphorescence emitters with denoted photophysical properties with respect to previous data reported in the literature.

Experimental section

General procedures

All manipulations have been performed under pre-purified N_2 using standard Schlenk techniques. Solvents have been distilled from appropriate drying agents. Commercial reagents 2-bromotriphenylene, 2-(diphenylphosphino) pyridine (PPyPh₂), KOH, and copper salts $[\text{Cu}(\text{MeCN})_4]\text{PF}_6$, $[\text{Cu}(\text{MeCN})_4]\text{OTf}$, $[\text{Cu}(\text{MeCN})_4]\text{BF}_4$ were purchased from Aldrich and used as received.

Physical measurements

Infrared spectra were recorded using a FT-IR 520 Nicolet Spectrophotometer. ^1H NMR (δ (TMS) = 0.0 ppm), $^{31}\text{P}\{^1\text{H}\}$ NMR (δ (85% H_3PO_4) = 0.0 ppm) and ^{19}F NMR spectra were recorded at 400 or 500 MHz using Varian and Bruker spectrometers at 25 °C (Centres Científics i Tecnològics, Universitat de Barcelona). J values are given in Hz. HR-ESI mass spectra have been recorded with a Thermo Fisher Scientific Orbitrap XL and a Bruker micrOTOF-Q mass spectrometer from acetonitrile solution. Absorption spectra were obtained in a 10 mm quartz cuvette in dichloromethane on a Varian Cary 100 Bio UV Spectrophotometer. The emission spectra of the compounds in solution were obtained in a fluorescence quartz cuvette of 10 mm path length, using a Horiba-JobinYvon SPEX Nanolog Spectrofluorimeter (Universitat de Barcelona). Quantum yields have been recorded on Absolute PL quantum yield spectrometer from Hamamatsu Photonics upon excitation the samples at 310-345 nm. Luminescence lifetimes were measured on a JYF-DELTAPRO-NL equipment upon excitation of the samples with a 284 nm NanoLED and collecting the decays through a bandpass filter of 400, 500, or 550 nm, depending on the emission maximum. The



best fittings correspond to biexponential decays, and the indicated values correspond to the average considering the respective amplitudes.

The single crystal X-ray data for all crystals were collected at 120 K using a Rigaku Synergy or Agilent SuperNova diffractometer both fitted with a HyPix-Arc 100 detector using mirror-monochromated Cu- $K\alpha$ ($\lambda = 1.54184 \text{ \AA}$) radiation. The structures were solved by intrinsic phasing (SHELXT)⁴³ and refined by full-matrix least squares on F^2 using Olex2,⁴⁴ utilizing the SHELXL module.⁴⁵ Anisotropic displacement parameters were assigned to non-H atoms and isotropic displacement parameters for all H atoms were constrained to multiples of the equivalent displacement parameters of their parent atoms with $U_{\text{iso}}(\text{H}) = 1.2 U_{\text{eq}}(\text{C})$ of their respective parent atoms. The experimental details for the data collections of [Au(L)(PPyPh₂), Cu1a, and Cu1b are given in Table S1. Deposition numbers 2481587, 2520370 and 2520371 contain the supplementary crystallographic data for this paper. These data are provided free of charge by the joint Cambridge Crystallographic Data Centre and Fachinformationszentrum Karlsruhe [Access Structures](#) service.

Synthesis and characterization

Synthesis of 2-ethynyltriphenylene (L)

The following synthesis has two parts: *First part:* 2-bromotriphenylene (0.500 g, 0.770 mmol), dichloridebis(triphenylphosphine)palladium (II) (0.054 g, 0.077 mmol) and triphenylphosphine (0.010 g, 0.038 mmol) were added in a Schlenk tube. Under nitrogen, a mix (4:1) of tetrahydrofuran (24 ml) and triethylamine (6 ml) was added. The resulting solution was stirred for 2h at 40°C. Next, copper (I) iodide (0.015 g, 0.077 mmol) was added to the Schlenk tube, and the resulting solution was stirred for 15 minutes at 40°C. Finally, ethynyltrimethylsilane (0.66 ml, 4.6 mmol) was added, and the resulting solution was stirred overnight at 60°C, and then at 85°C for 4h. The reaction mixture was allowed to reach room temperature, and the volatiles were removed under vacuum. The solid obtained was purified through a chromatographic column as follows: a first column where stationary phase was silica, and the eluent was a mix (1:1) of hexane and dichloromethane. This column was used as precolumn to separate the palladium residues. A second column where stationary phase was silica, and the eluent was a mixture (9:1) of hexane and dichloromethane. This second column allowed the separation of the desired product: trimethyl (triphenylen-2-ylethynyl)



silane. *Second part:* trimethyl (triphenylen-2-ylethynyl) silane (0.095 g, 0.290 mmol) was dissolved in a mix (1:2) of methanol (10 ml) and tetrahydrofuran (20 ml) in a Schlenk tube. Potassium fluoride dihydrate (0.191 g, 2.03 mmol) was added to the Schlenk tube, and the resulting solution was stirred for 2h at room temperature. The volatiles were removed under vacuum. Then, organic phase was extracted with dichloromethane, washed with water, and dried with anhydrous magnesium sulfate. The reaction mixture was filtered. The whitish solid obtained was dried under vacuum: 2-ethynyltriphenylene. Yield: 93%. IR ($\bar{\nu}$, cm^{-1}): 3265 (ν C \equiv CH), 2959 (ν CH), 2160 (ν C \equiv C), 1488 (δ CH). δ_{H} (400 MHz, CDCl_3) 8.82 (d, $J = 1.6$, 1H, H_{I}), 8.68–8.58 (m, 5H, $H_{3\text{-}H_{\text{II}}}$), 7.75 (dd, $J = 8.5$, $J = 1.6$, 1H, H_2), 7.72–7.64 (m, 4H, $H_{3\text{-}H_{\text{II}}}$), 3.23 (s, 1H, (CCH (ethynyl))).

Synthesis of the Au(I) complexes

Synthesis of [AuCl(PPyPh₂)]. Diphenyl-2-Pyridyl Phosphane (PPyPh₂) (0.212 g, 0.81 mmol) and [AuCl(tht)] (0.259 g, 0.81 mmol) were dissolved in 5 mL of dichloromethane and stirred for 1h at RT, the resultant mixture was precipitated by adding 10 ml of hexane and filtrated via cannula to get the desired product. Yield: 92%. IR ($\bar{\nu}$ cm^{-1}): 3058 (ν CH), 1568 (ν C=N), 1477 (ν C=C), 1311 (ν CN), 1176 + 1157 (δ P-Ph). δ_{H} (400 MHz, CDCl_3) 8.79 (d, $J = 4.7$, 0.9, 1H, H_{a}), 7.99 (t, $J = 7.8$, 1.1, 1H, H_{d}), 7.83–7.77 (m, 1H, H_{c}), 7.74–7.65 (m, 4H, Ph), 7.56–7.43 (m, 6H, Ph), 7.42–7.37 (m, 1H, H_{b}). δ_{P} (162 MHz, CDCl_3) 32.3.

Synthesis of [Au(L)(PPyPh₂)]. 2-ethynyl triphenylene (L) (0.051 g, 0.20 mmol) was added to a methanol (10 mL) solution of KOH (0.023 g, 0.40 mmol). The mixture was stirred for 2 h at RT. Then, a solution of [AuCl(PPyPh₂)] (0.100 g, 0.20 mmol) in 10 mL of dichloromethane was slowly added. The solution was left overnight with rigors stirring at RT after which the solvents were removed under vacuum. The mixture was vacuum dried and then dissolved in minimal amount of dichloromethane to pass it through celite, the filtrate from the celite column was dried to a minimal amount and 5 mL of diethyl ether was added to precipitate the white solid of complex. Yield: 58%. IR ($\bar{\nu}$ cm^{-1}): 3051 (ν CH), 2112 (ν C \equiv C), 1604 (ν C=C), 1569 (ν C=N), 1480-1446 (δ CH), 1182 (ν CN), 1099 (δ CN), 1045 + 1030 (δ CH). δ_{H} (400 MHz, CDCl_3) 8.85 (d, $J = 1.6$, 1H, H_{I}), 8.81 (d, $J = 4.7$, 1H, H_{a}), 8.67–8.58 (m, 4H, $H_{4\text{-}H_{\text{II}}}$), 8.55 (d, $J = 7.8$, 1H, H_3), 8.08 (t, $J = 1.1$, 1H, H_{d}), 7.84–7.73 (m, 6H, H_{c} , H_2 , Ph), 7.68–7.60 (m, 4H, $H_{4\text{-}H_{\text{II}}}$), 7.56–7.44 (m, 6H, Ph), 7.42–7.36 (m, 1H, H_{b}). δ_{P}



(162 MHz, CDCl₃) 41.3. ESI-MS (+) *m/z*: (Lp = PPyPh₂, L = chromophore ligand C₂₀H₁₁): 1171.191 [2M-Lc]⁺, 501.079 [(Lp)Au(ACN)]⁺, 723.139 [(Lp)₂Au]⁺, 1434.278 [(Lp)₃Au₂(L)]⁺, 1883.332 [(Lp)₃Au₃(L)₂]⁺.

Synthesis of the Au(I)-Cu(I) complexes

[Au₂Cu₂(L)₂(PPyPh₂)₂][PF₆]₂ (Cu1a). [Au(L)(PPyPh₂)] (0.020 g, 0.028 mmol) was added in 3 mL of dichloromethane and stirring for 5 min. Then [Cu(MeCN)₄]PF₆ (0.011 g, 0.028 mmol) previously dissolved in 2 mL of dichloromethane was added. The addition of [Cu(MeCN)₄]PF₆ causes a sudden change of colour to bright orange. After overnight rigors stirring, the solution was dried under vacuum and the residue was dissolved in 2 mL of dichloromethane and precipitated by 4 mL of hexane. Complex Cu1a was obtained as a light orange solid. Yield: 85%. IR ($\bar{\nu}$ cm⁻¹): 3082 + 2965 (ν CH), 2217 (ν C≡C), 1670 (ν C=N), 1607 (ν C=C), 1485 + 1438 (δ CH), 1285 + 1261 (ν CN), 833 (ν PF). δ_{H} (400 MHz, CD₃COCD₃) 9.55 (d, *J* = 5.3, 2H), 8.97–8.64 (m, 2H), 8.50–8.28 (m, 4H), 8.18–7.97 (m, 4H), 7.94–7.63 (m, 41H), 7.59–7.31 (m, 6H). δ_{P} (162 MHz, CD₃COCD₃) 47.4, -144.3 (hept, *J* = 707). δ_{F} (376 MHz, CDCl₃) -67.3 (d, *J* = 707). ESI-MS (+) *m/z*: (Lp = PPyPh₂, L = chromophore ligand C₂₀H₁₁): 1695.102 [M - PF₆]⁺, 590.013 [(Lp)AuCu(ACN)(CN)]⁺, 723.140 [(Lp)₂Au]⁺, 1035.043 [(Lp)₂Au₂Cu(CN)₂]⁺, 1485.211 [(Lp)₂Au₂(L)₂Cu], 2197.353 [(Lp)₃Au₃(L)₃Cu]⁺. HR ESI-MS: 1693.1019 [M - PF₆]⁺, calculated for C₇₄H₅₀N₂P₃Cu₂Au₂F₆: 1693.1009.

[Au₂Cu₂(L)₂(PPyPh₂)][OTf]₂ (Cu1b). [Au(L)(PPyPh₂)] (0.020 g, 0.028 mmol) was added in 3 mL of dichloromethane to stir for 5 min. Then [Cu(MeCN)₄]OTf (0.012 g, 0.028 mmol) previously dissolved in 2 mL of dichloromethane was added. The addition of [Cu(MeCN)₄]OTf causes a sudden change of color to bright orange. After 4h of rigors stirring, the solution was dried under vacuum. The solid was dissolved in 2 mL of dichloromethane and precipitated with 4 mL of hexane. Complex Cu1b was obtained as a brown solid. Yield: 80%. IR ($\bar{\nu}$ cm⁻¹): 3072 (ν CH), 1938 (ν C≡C), 1610 (ν C=N), 1586 (ν C=C), 1482-1436 (δ CH), 1223 (ν CF), 1158 (ν CN), 1023 (ν S=O). δ_{H} (400 MHz, CDCl₃) 9.76 (s, 2H), 8.74–8.57 (m, 4H), 8.52 (d, *J* = 7.9, 2H), 8.24 (d, *J* = 8.6, 2H), 8.15 (s, 4H), 7.92 (s, 2H), 7.84–7.58 (m, 10H), 7.76–7.61 (m, 15H), 7.20–6.82 (m, 8H). δ_{P} (162 MHz, CDCl₃) 41.9. δ_{F} (376 MHz, CDCl₃) -77.9. ESI-MS (+) *m/z*: (Lp = PPyPh₂, L = chromophore ligand



$C_{20}H_{11}$): 1699.099 $[M - OTf]^+$, 590.016 $[(Lp)_2AuCu(ACN)(CN)]^+$, 723.143 $[(Lp)_2Au]^+$, 815.100 $[(Lp)Au(L)Cu(ACN)]^+$, 1171.199 $[(Lp)_2Au_2(L)]^+$, 1485.216 $[(Lp)_2Au_2(L)_2Cu]^+$, 2197.353 $[(Lp)_3Au_3(L)_3Cu]^+$. HR ESI-MS: 1697.0881 $[M - OTf]^+$, calculated for $C_{75}H_{50}N_2P_2Cu_2Au_2F_3SO_3$: 1697.0887.

$[Au_2Cu_2(L)_2(PPyPh_2)_2][BF_4]_2$ (**Cu1c**). A similar procedure used for complex Cu1a was followed for the synthesis of complex Cu1c, but using $[Cu(MeCN)_4]BF_4$ instead of using $[Cu(MeCN)_4]PF_6$. Complex was obtained as a red solid. Yield: 95%. IR ($\bar{\nu}$ cm^{-1}): 3075 (ν CH), 1974 (ν $C\equiv C$), 1609 + 1587 (ν $C=N$), 1482 (ν $C=C$), 1287 (δ CH), 1052 + 633 + 617 (ν BF). δ_H (400 MHz, CD_3COCD_3) 9.36 (s, 1H), 8.66 (d, $J = 8.0$, 3H), 8.56 (d, $J = 7.9$, 2H), 8.45–8.36 (m, 2H), 8.19 (d, $J = 8.6$, 4H), 7.93–7.77 (m, 4H), 7.74–7.24 (m, 41H). δ_P (162 MHz, CD_3COCD_3) 47.0. δ_F (376 MHz, CD_3COCD_3) -150.4. ESI-MS (+) m/z : (Lp = PPyPh₂, L = chromophore ligand $C_{20}H_{11}$): 1637.146 $[M - BF_4]^+$, 590.014 $[(Lp)AuCu(ACN)(CN)]^+$, 723.141 $[(Lp)_2Au]^+$, 1035.044 $[(Lp)_2Au_2Cu(CN)_2]^+$, 1485.211 $[(Lp)_2Au_2(Lc)_2Cu]^+$, 2197.353 $[(Lp)_3Au_3(L)_3Cu]^+$. HR ESI-MS: 1635.1396 $[M - BF_4]^+$, calculated for $C_{74}H_{50}N_2P_2Cu_2Au_2BF_4$: 1635.1408.

Preparation of doped matrixes

The complex-doped film was prepared by drop-casting a mixture of the complex and the corresponding polymer onto a quartz substrate, as detailed below:

to prepare the polymer solution, PMMA (MW: 97,000) or PS (MW: 280000) was dissolved in chloroform at a concentration of 200 mg/mL. Subsequently, to a 50 μ L of polymer solution was added to the same volume of a solution of the sample at a concentration of 2 mM. The films were drop cast onto a quartz substrate at room temperature to avoid any thermal annealing.

Supporting Information

Characterization data (NMR, IR, mass spectra); X-ray crystallographic information and packing; Photophysical information containing emission quantum yields, lifetimes and absorption and emission complementary figures.



Conflicts of interest

There are no conflicts to declare.

Acknowledgements

The authors are grateful to Projects PID2022-139296NB-I00 funded by the Ministerio de Ciencia, Innovación y Universidades of Spain MCIU/AEI/10.13039/501100011033 and FEDER, UE. This article is based upon work from COST Action CA22131, LUCES Supramolecular LUminescent Chemosensors for Environmental Security, supported by COST (European Cooperation in Science and Technology). Also acknowledges IFARHU-SENACYT program in Panamá for the grant no. 270-2022-112 as Ph.D. Scholarship.



References

- 1 A. V. Artem'ev, M.P. Davydova, L.S. Klyushova, E.H. Sadykov, M.I. Rakhmanova, T.S. Sukhikh, *Dalton Trans.*, 2024, **53**, 18027.
- 2 C. Sun, B.K. Teo, C. Deng, J. Lin, G.-G. Luo, C.-H. Tung, D. Sun, *Coord. Chem. Rev.* 2021, **427**, 213576.
- 3 C.-H. Huang, M. Yang, X.-L. Chen, C.-Z. Lu, *Dalton Trans.*, 2021, **50**, 5171.
- 4 J. R. Shakirova, E.V. Grachova, V.V. Gurzhiy, S. Kumar Thangaraj, J. Jānis, A.S. Melnikov, A.J. Karttunen, S.P. Tunik, I.O. Koshevoy, *Angew. Chem. Int. Ed.* 2018, **57**, 14154.
- 5 M. Casciotti, G. Romo-Islas, M. Álvarez, F. Molina, J.M. Muñoz-Molina, T. R. Belderrain, L. Rodríguez, *Dalton Trans.*, 2022, **51**, 17162.
- 6 A. Pinto, J.S. Ward, K. Rissanen, M. Smith, L. Rodríguez, *Dalton Trans.*, 2022, **51**, 8795.
- 7 R. K. Gupta, Z. Wang, B. Mohan, C.-H. Tung, D. Sun, *Adv. Funct. Mater.* 2025, **35**, 2507047
- 8 A. de Aquino, N. Santamaria, A.J. Moro, D. Aguilà, A. Prieto, M.C. Nicasio, J.C. Lima, L. Rodriguez, *Inorg. Chem.* 2025, **64**, 3392.
- 9 A. Frontera, L. Rodríguez, *Adv. Inorg. Chem.* 2024, **84**, 55.
- 10 J.C. Lima, L. Rodríguez, *Adv. Organomet. Chem.* 2025, **83**, 139.
- 11 S. Sculfort, P. Braunstein, *Chem. Soc. Rev.*, 2011, **40**, 2741.
- 12 P. Ai, M. Mauro, L. De Cola, A.A. Danopoulos, P. Braunstein, *Angew. Chem. Int. Ed.* 2016, **55**, 3338.
- 13 Q.-C. Peng, Y.-B. Si, Z.-Y. Wang, S.-H. Dai, Q.-S. Chen, K. Li, S.-Q. Zang, *ACS Cent. Sci.* 2023, **9**, 1419.
- 14 X. Zhang, H. Xu, *Angew. Chem. Int. Ed.* 2024, **63**, e202317597.
- 15 X.-H. Ma, J. Li, P. Luo, J.-H. Hu, Z. Han, X.-Y. Dong, G. Xie, S.-Q. Zang, *Nature Commun.* 2023, **14**, 4121.
- 16 W.-Q. Shi, L. Zeng, R.-L. He, X.-S. Han, Z.-J. Guan, M. Zhou, Q.-M. Wang, *Science* 2024, **383**, 326.
- 17 G. Romo-Islas, J.S. Ward, K. Rissanen, L. Rodriguez, *Inorg. Chem.* 2023, **62**, 8101.
- 18 I.O. Koshevoy, Y.-C. Chang, A. J. Karttunen, M. Haukka, T. Pakkanen, P.-T. Chou, *J. Am. Chem. Soc.* 2012, **134**, 6564



- 19 A. Yu. Baranov, S.O. Slavova, A.S. Berezin, S.K. Petrovskii, D. G. Samsonenko, I. Yu. Bagryanskaya, V.P. Fedin, E.V. Grachova, A.V. Artem'ev, *Inorg. Chem.* 2022, **61**, 10925.
- 20 M. Dahlen, E.H. Hollesen, M. Kehry, M. T. Gamer, S. Lebedkin, D. Schooss, M.M. Kappes, W. Klopffer, P.W. Roesky, *Angew. Chem. Int. Ed.* 2021, **60**, 23365.
- 21 A.P. Atencio, S. Burguera, G. Zhuchkov, A. de Aquino, J.S. Ward, K. Rissanen, J.C. Lima, I. Angurell, A. Frontera, L. Rodríguez, *Inorg. Chem. Front.*, 2025, **12**, 3041.
- 22 W.-H. Yu, C. Chen, P. Hu, B.-Q. Wang, C. Redshaw, K.-Q. Zhao, *RSC Adv.*, 2013, **3**, 14099.
- 23 M. Powers, R. J. Twieg, J. Portman, B. Ellman, *J. Chem. Phys.* 2022, **157**, 134901.
- 24 S. Keller, F. Brunner, A. Prescimone, E. C. Constable, C. E. Housecroft, *Inorg. Chem. Commun.* 2015, **58**, 64.
- 25 Ferrer, A. Gallen, A. Gutiérrez, M. Martínez, E. Ruiz, Y. Lorenz, M. Engeser, *Chem. Eur. J.* 2018, **57**, 7346-7354.
- 26 R. Nandy, S. Sankararaman, *Beilstein J. Org. Chem.*, 2010, **6**, 992.
- 27 G.F. Manbeck, W.W. Brennessel, R.A. Stockland, Jr., R. Eisenberg. *J. Am. Chem. Soc.* 2010, **132**, 12307.
- 28 F. Liu, G. Cao, Z. Feng, Z. Cheng, Y. Yan, Y. Xu, Y. Jiang, Y. Chang, Y. Lv and P. Lu, *ACS Appl. Mater. Interfaces*, 2023, **15**, 47307.
- 29 M. Ikeda, M. Takeuchi and S. Shinkai, *Chem. Commun.*, 2003, **3**, 1354.
- 30 R. Nandy and S. Sankararaman, *Org. Biomol. Chem.*, 2010, **8**, 2260.
- 31 S. K. Petrovskii, A. V. Paderina, A. A.Sizova, A. Y. Baranov, A A. Artem'ev, V. V.Sizov, E. V. Grachova, *Dalton Trans.* 2020, **49**, 13430.
- 32 S. Nayeri, S. Jamali, A. Jamjah, H. Samouei, *Inorg. Chem.* 2019, **58**, 12122.
- 33 G. Romo-Islas, S. Burguera, A. Frontera and L. Rodríguez, L, *Inorg. Chem.* 2024, **63**, 2821–2832.
- 34 A. de Aquino; F. J. Caparrós, G. Aullón; K. N. Truong, K. Rissanen, J.C Lima and L. Rodríguez, *Dalton Trans.*, 2022, **51**, 16282–16291.
- 35 A. P. Atencio, A. Sevillano, A. Lázaro, Z. Freixa, D. Aguilà, I. Angurell, L. Rodríguez, *New J. Chem.*, 2025, **49**, 18716.



- 36 A. de Aquino, F. J. Caparrós, G. Aullón, J. S. Ward, K. Rissanen, Y. Jung, H. Choi, J. C. Lima and L. Rodríguez, *Chem. – Eur. J.*, 2021, **27**, 1810.
- 37 A. Pinto, A. Llanos, R.M. Gomila, A. Frontera, L. Rodriguez. *Inorg. Chem.* 2023, **62**, 7131.
- 38 R. Donamaria, V. Lippolis, J.M. López de Luzuriaga, M. Monge, M. Nieddu, M.E. Olmos, *Inorg. Chem.* 2018, **57**, 11099.
- 39 I.S. Krytchankou, D.V. Krupenya, A.J. Karttunen, S.P. Tunik, T.A. Pakkanen, P.-T. Chou, I.O. Koshevoy, *Dalton Trans.*, 2014, **43**, 3383.
- 40 X.-Y. Chang, G.-T. Xu, B. Cao, J.-Y. Wang, J.-S. Huang, C.-M. Che, *Chem. Sci.*, 2017, **8**, 7815.
- 41 O. Crespo, M.C. Gimeno, A. Laguna, F.J. Lahoz, C. Larraz, *Inorg. Chem.* 2011, **50**, 9533.
- 42 S. Nayeri, S. Jamali, A. Jamjah, J.R. Shakirova, S.P. Tunik, V. Gurzhiy, H. Samouei, H.R. Shahsavari, *Inorg. Chem.* 2020, **59**, 5702.
- 43 G. M. Sheldrick, *Acta Crystallogr. Sect. A Found. Adv.*, 2015, **71**, 3.
- 44 O. V. Dolomanov, L. J. Bourhis, R. J. Gildea, J. A. K. Howard, H. Puschmann, *J. Appl. Crystallogr.* 2009, **42**, 339.
- 45 G. M. Sheldrick, *Acta Crystallogr. Sect. C, Struct. Chem.* 2015, **71**, 3.



The data supporting the findings of this study, including synthetic procedures, spectroscopic data (NMR, IR, MS), photophysical measurements, and crystallographic information, are available within the article and its Supplementary Information. Crystallographic data for compounds **[Au(L)(PPyPh₂)]**, **Cu1a**, and **Cu1b** have been deposited at the Cambridge Crystallographic Data Centre (CCDC) under accession numbers 2481587, 2520370 and 2520371 and can be obtained from <https://www.ccdc.cam.ac.uk/structures>.

View Article Online
DOI: 10.1039/D6DT00964F

